Nat Hazards (2014) 74:1141–1161
DOI 10.1007/s11069-014-1234-0

ORIGINAL PAPER

A prediction model for debris flows triggered by a runoff-induced mechanism

Bin Yu · Yuan Zhu · Tao Wang · Yuanjing Chen · Yunbo Zhu · Yongbo Tie · Ke Lu

Received: 26 December 2013 / Accepted: 11 May 2014 / Published online: 17 May 2014

Abstract Many debris flows were triggered within and also outside the Dayi area of the Guizhou Province, China, during a rainstorm in 2011. High-intensity short-duration rainfall was the main triggering factor for these gully-type debris flows which are probably triggered by a runoff-induced mechanism. A revised prediction model was introduced for this kind of gully-type debris flows with factors related to topography, geology, and hydrology (rainfall) and applied to the Wangmo River catchment. Regarding the geological factor, the "soft lithology" and "loose sediments" in the channel were added to the list of the average firmness coefficient for the lithology. Also, the chemical weathering was taken into account for the revised geological factor. Concerning the hydrological factor, a coefficient of variation of rainfall was introduced for the normalization of the rainfall factor. The prediction model for debris flows proposed in this paper delivered three classes of the probability of debris flow occurrence. The model was successfully validated in debris flow gullies with the same initiation mechanism in other areas of southwest China. The generic character of the model is explained by the fact that its factors are partly based on the initiation mechanisms and not only on the statistical analyses of a unique variety of local factors. The research provides a new way to predict the occurrence of debris flows initiated by a runoff-induced mechanism.

Keywords Prediction model · Debris flow · Runoff · Rainstorm · Dayi

B. Yu (✉) · Y. Zhu · T. Wang · Y. Chen · Y. Zhu
State Key Laboratory of Geohazard Prevention and Geoenvironment Protection, Chengdu University of Technology, Chengdu 610059, China
e-mail: drbinyu@yahoo.com

Y. Tie
Chengdu Institute of Geology and Mineral Resources, China Geological Survey, Chengdu 610081, China

K. Lu
Sichuan Institute of Geological Engineering Investigation, Chengdu 610072, China

1 Introduction

During a rainstorm from June 5 to June 6, 2011, many debris flows were triggered within and outside the Dayi area in the Guizhou Province of China. These debris flows were gully-type debris flows, which are dangerous and cause enormous risks (Yu et al. 2013b). Gully-type debris flows occur in areas with significant gully topography (Liu et al. 2009). The gully-type debris flows in the study area were triggered partly by flash floods causing a runoff-induced effect (Kean et al. 2013), and partly by the development of many shallow landslides. Debris flow initiation is typically attributed to runoff from low-permeability surfaces during rain storms, which at a critical discharge threshold mobilize loose sediments which can transform into a debris flow (Kean et al. 2013). The initiation of a debris flow by a runoff effect can be facilitated by the accumulation in very steep channels of abundant solid materials from old landslide debris, soil, talus, or dumped material deposits. Kean et al. (2013) pointed out that the mechanistic theories for debris flow initiation by runoff are grouped into two categories: (1) mass failure of the channel sediment by a sliding along a discrete failure plane: a sudden large impulse of sediment to be added to and/or entrained within the water flow, such as from the failure of the sediment-filled bed of the channel or the failure of the channel banks caused by channel erosion, and (2) grain-by-grain bulking by hydrodynamic forces: a critical discharge of water creating a debris flow surge by eroding the sediment by hydrodynamic forces from the top down rather than by sliding at a failure plane at a depth of several until many grains below the surface. High-speed water flows generated during unusually intense rainstorms can create also an extra shear force of the rushing water along steep slopes. In addition to the component of the driving force induced by the weight of the sediment, it may destabilize the material and initiate a debris flow (Johnson and Rodine 1984).

To mitigate and prevent hazards induced by debris flows and related risks, one must understand the formation of these in order to make reliable forecasts. Many factors are related to the occurrence of debris flows such as the basin gradient, the percentage of basin area with slopes greater than or equal to 30 %, basin ruggedness, additional measures of gradient, slope aspect, rainfall intensity, and soil properties, including the clay percentage, the percentage of organic matter, the soil granulometry and sorting, and the soil liquid limit (Cannon et al. 2010). Liu et al. (2009) among others stated that there are three groups of factors playing a major role in the formation of ordinary gully-type debris flows. They are related to topography, geology, and hydrology.

Yu et al. (2013b) introduced a formation model for gully-type debris flows for the Chenyoulan River Watershed with factors related to topography, geology, and rainfall. Their model consists of three critical values to make four classes of the probability of debris flow occurrence. The model used a limited number of lithological classes, which makes it less applicable for other areas. For the assessment of the geological factor, the chemical weathering was not considered as well as the presence of loose sediments in catchments, deposited by landslides triggered by a strong earthquake (Yu et al. 2013c). Because of the scarcity of detailed rainfall data in their research area, only the average annual rainfall was used to normalize the rainfall data for the rainfall factor, which decreases also the applicability of the model in other areas.

Therefore, in this study, a refined geological factor is introduced by including a so-called firmness coefficient for very soft rock and for landslide deposits and loose sediments in channels, and by taking into account the degree of chemical weathering. Also, a variety coefficient of the 10-min rainfall intensity is introduced for the normalization of the rainfall factor. The revised prediction model for debris flows with a runoff-induced mechanism

will be calibrated on debris flows which occurred in 2011 in the Dayi area. The model will be validated on debris flows, which were triggered in a number of selected regions in southwest China.

2 Description of the Dayi study area

The calibration area with 66 gullies is located downstream of Dayi town (see Fig. 1). It is crossed in a north–south direction by the Wangmo River, a main branch of the Nanpanjiang River, which is one of the branches of the Zhujiang River, the third large river in China. The lowest place in the study area is 710 m in altitude, and the highest peaks in the catchment have altitudes between 1,500 and 1,600 m. The channel gradients in the upstream part of the gullies are very large, and some of them are larger than 35°. These are suitable topographic conditions for debris flow outbreaks. But above a critical slope gradient (around 35°), there is no solid source material to initiate debris flows by concentrated flash floods. There are only two lithological units in the calibration area: hard siltstones interbedded with thin mudstones. The thickness ratio of siltstone and mudstone is 3–4 to 1. There is no fault in the study area. The statistics of historical earthquakes give the study area a general seismic intensity of VI (NSBC 1990).

The average annual rainfall lies in a range between 1,210 and 1,320 mm, and the average annual temperature varies between 14.4 and 16 °C. Figure 2 shows the rainfall figures of the Dayi and Xintun (13.1 km in the south of Dayi) stations, before and after the outbreak of the debris flows from June 5 until June 6, 2011. The rainfall started at 22:00, June 5, at the Dayi station, while there was almost no rainfall at the Xintun station until 1:00, June 6. The maximum hourly rainfall was 105.9 mm at the Dayi station from 23:00 to 24:00, June 5. The debris flows were triggered during this period. The rainfall data for the 66 gullies, including the hourly rainfall, and cumulative rainfall before the triggering of the debris flows were obtained by interpolation of the rainfall data of the Dayi and Xintun stations (see Table 1).

3 The classification of the gullies in the Dayi study area

Field investigations were conducted in the 66 gullies of the study area. Debris flow activity during the heavy rain storm of June 5 to June 6, 2011, was observed in 47 gullies. Some debris flows were triggered by a runoff-induced mechanism, some were initiated by shallow landslides, and some were triggered by both processes. In this study, we will only focus on debris flows which were triggered by a runoff-induced mechanism. We distinguished three classes related to the presence or absence of debris flows in gullies: (1) There are 22 gullies classified as "no debris flow," which means there were no debris flows or debris flows that originated solely from shallow landslides because there was no material entrained in the channels. (2) There are 25 gullies classified as "debris flow" with obvious material entrained in the channels, which means that the presence of debris flows is caused by a runoff-induced mechanism, or by *both* a runoff-induced mechanisms and shallow landslides. (3) There are 19 gullies classified as "uncertain" without clear indications of entrainment of material in the channels; debris flows and shallow landslides are present, but it is not sure whether the debris flows are triggered by a runoff-induced mechanism. Figure 1 shows the location of the gullies subdivided into three classes according to the above given definitions. Table 1 gives for each gully the classification together with the

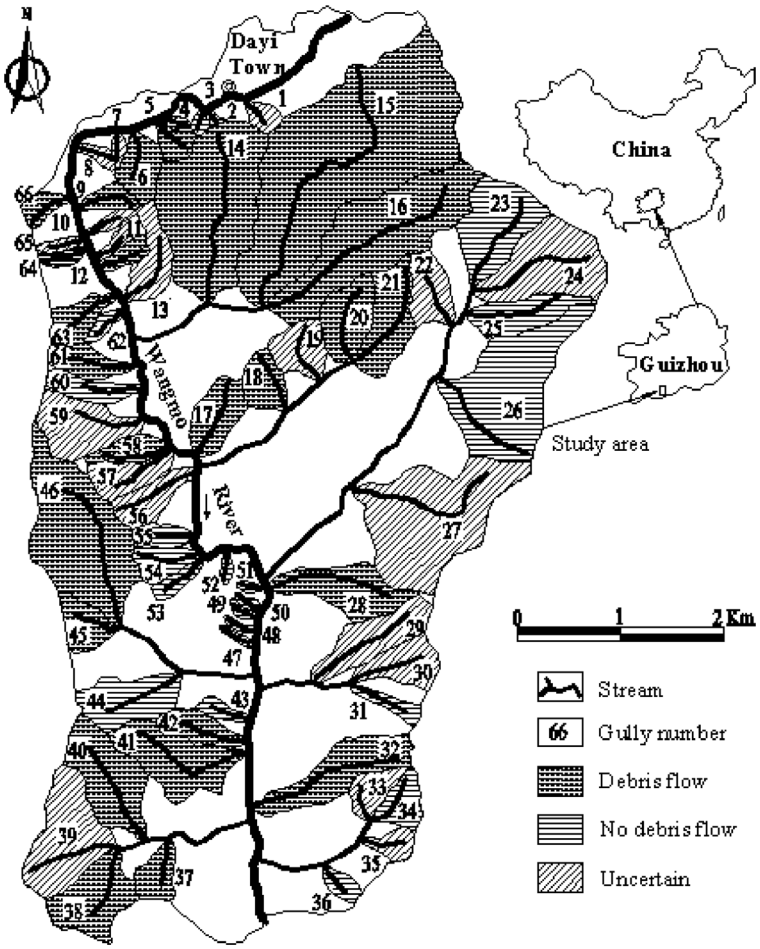

Fig. 1 The classification of the investigated gullies in Dayi area, in the Guizhou Province

parametric values related to the three revised debris flow prediction factors, which will be described shortly in the next paragraph.

4 The prediction factors of debris flows with a runoff-induced mechanism

The basic ideas behind the three prediction factors used in this study are the same as those in Yu et al. (2013b), but there are, as explained above, some refinements of the geological and the rainfall factor.

4.1 The topographic factor

Yu et al. (2011, 2013b) obtained a dimensionless topographic factor describing the role of topography in the formation of debris flows with a runoff-induced mechanism (Eq. 1):

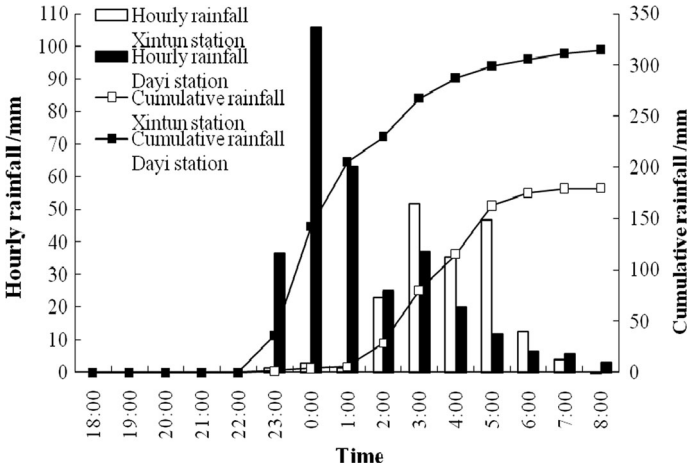

Fig. 2 Rainfall characteristics in the Dayi area from June 5 to June 6, 2011

$$T = FJ(A/A_0)^{0.2} = J(A/L^2)(A/A_0)^{0.2} \quad (1)$$

in which T is the dimensionless topographic factor of the source (formation) section of the gully where the debris flows are initiated; F (=A/L^2) is the form factor with A: the area (km^2) and L (km): the length of the channel in the source section. J is the average slope of the channel; A_0 is the unit area of the gully in the source section (=1 km^2).

The topographic factor includes the form factor, the average slope, and the area of catchment of the formation area. The form factor is highly related to the distribution of the hydrograph: a larger form factor produces a larger discharge and velocity than a smaller form factor. The discharge of the flow is the key triggering factor for debris flows with a runoff-induced mechanism. Therefore, under the same conditions, a watershed area with a large form factor has a higher likelihood to generate debris flows (Chang 2007). The parameters related to the average slope and the area of the catchment also influence the surface flow discharge and the flow velocity and thus the resulting downslope movement of sediments.

The topographic factors were calculated using a 1:10.000 topographic map. The values of the topographic factor T for all the 66 gullies are listed in Table 1.

4.2 The geological factor

Yu et al. (2012, 2013b) obtained a dimensionless geological factor to represent the role of geology in the formation of debris flows triggered by flash floods in channels. The geological factor contains a firmness coefficient (F_0) for the lithology and some correction coefficients. Yu et al. (2013a) extended the geological factor with more lithological units such as the soft rock (with an average firmness coefficient $2 \geq F_0 \geq 1.5$) and the loose sediments in the channel (with an average firmness coefficient $F_0 < 1$) (see Table 2). The chemical weathering was also taken into account for the revised geological factor (Eq. 2):

$$G = F_0 C_1 C_2 C_3 C_4 \quad (2)$$

in which G is the dimensionless geological factor; F_0 is the average firmness coefficient of the lithology in the source section of the gully; C_1 is a correction coefficient for seismic

Table 1 Parametric values related to different debris flow prediction factors and the presence of debris flows in gullies in the Dayi area. (For an explanation see text)

No.	J	F	A (km^2)	Lithology	R_0 (mm)	B (mm)	I (mm)	T	G	R	P	Debris
1	0.377	0.893	0.04	SIS[#]	1320	139.5	103.7	0.177	7.11	2.719	0.721	Uncertain
2	0.452	0.505	0.012	SIS	1320	138.2	102.8	0.094	7.11	2.695	0.630	No
3	0.433	0.73	0.014	SIS	1320	138	102.6	0.135	7.11	2.691	0.676	No
4	0.449	0.573	0.014	SIS	1320	138	102.7	0.109	7.11	2.692	0.648	Yes
5	0.22	0.714	0.062	SIS	1320	136.1	101.2	0.09	7.11	2.654	0.615	Yes
6	0.36	0.753	0.084	SIS	1320	134.1	99.69	0.165	7.11	2.614	0.684	Yes
7	0.621	0.517	0.019	SIS	1320	134.9	100.3	0.146	7.11	2.63	0.671	Uncertain
8	0.485	0.446	0.032	SIS	1320	134.4	99.94	0.109	7.11	2.621	0.630	Uncertain
9	0.438	0.305	0.046	SIS	1320	130.2	96.8	0.072	7.11	2.538	0.563	Yes
10	0.702	0.559	0.037	SIS	1320	127.7	94.9	0.203	7.11	2.488	0.678	Uncertain[$]
11	0.541	0.557	0.037	SIS	1320	125.7	93.47	0.156	7.11	2.451	0.634	Uncertain
12	0.585	0.444	0.042	SIS	1320	124.2	92.36	0.138	7.11	2.422	0.611	Yes
13	0.511	0.53	0.066	SIS	1320	121.5	90.3	0.157	7.11	2.368	0.613	Uncertain
14	0.137	1.163	1.218	SIS	1320	129.6	96.39	0.166	7.11	2.527	0.662	Yes
15	0.132	0.579	2.257	SIS	1320	134.9	100.3	0.09	7.11	2.631	0.609	Yes
16	0.253	0.426	1.014	SIS	1320	125.7	93.42	0.108	7.11	2.45	0.589	Yes
17	0.487	0.626	0.178	SIS	1280	108.6	80.7	0.216	7.11	2.182	0.602	Yes
18	0.296	0.473	0.188	SIS	1280	111.9	83.2	0.100	7.11	2.249	0.532	Yes
19	0.189	0.488	0.253	SIS	1280	114.5	85.1	0.070	7.11	2.301	0.507	Uncertain
20	0.180	0.478	0.276	SIS	1280	117.6	87.4	0.066	7.11	2.364	0.516	Yes
21	0.160	0.388	0.236	SIS	1280	119.6	88.9	0.046	7.11	2.403	0.488	Yes
22	0.548	1.123	0.215	SIS	1280	121.5	90.3	0.453	7.11	2.442	0.782	Uncertain
23	0.526	0.731	0.222	SIS	1280	127.5	94.8	0.284	7.11	2.564	0.748	No
24	0.293	0.668	0.698	SIS	1280	125.8	93.5	0.183	7.11	2.528	0.675	Uncertain
25	0.450	0.649	0.288	SIS	1280	120.2	89.4	0.228	7.11	2.417	0.674	No

Table 1 continued

No.	J	F	A (km^2)	Lithology	R_0 (mm)	B (mm)	I (mm)	T	G	R	P	Debris
26	0.309	0.752	1.139	SIS	1280	115.2	85.6	0.238	7.11	2.316	0.652	No
27	0.272	0.931	1.367	SIS	1280	100.0	74.3	0.270	7.11	2.009	0.580	Uncertain
28	0.361	0.437	0.255	SIS	1220	92.5	68.7	0.120	7.11	1.950	0.478	Yes
29	0.366	0.699	0.395	SIS	1220	86.5	64.2	0.212	7.11	1.823	0.501	Uncertain
30	0.493	0.724	0.201	SIS	1220	83.7	62.1	0.259	7.11	1.763	0.505	Uncertain
31	0.638	0.443	0.098	SIS	1220	80.8	60.0	0.177	7.11	1.702	0.452	No
32	0.349	0.319	0.368	SIS	1210	73.0	54.1	0.091	7.11	1.548	0.360	Yes
33	0.310	1.928	0.129	SIS	1210	69.6	51.6	0.396	7.11	1.476	0.460	Uncertain
34	0.620	1.294	0.148	SIS	1210	70.0	51.9	0.548	7.11	1.484	0.494	No
35	0.660	0.613	0.062	SIS	1210	65.5	48.5	0.232	7.11	1.389	0.389	Uncertain
36	0.673	0.655	0.067	SIS	1210	61.6	45.7	0.256	7.11	1.307	0.373	No
37	0.467	0.894	0.133	SIS	1210	62.5	46.3	0.279	7.11	1.326	0.385	Yes
38	0.175	1.637	0.341	SIS	1210	59.5	44.1	0.231	7.11	1.261	0.353	Yes
39	0.541	1.54	0.210	SIS	1210	66.3	49.2	0.610	7.11	1.407	0.478	Uncertain
40	0.419	0.76	0.500	SIS	1210	68.1	50.5	0.277	7.11	1.444	0.419	Yes
41	0.466	1.88	0.243	SIS	1210	72.8	54.0	0.661	7.11	1.544	0.533	Yes
42	0.512	0.595	0.109	SIS	1210	75.8	56.2	0.195	7.11	1.609	0.435	Yes
43	0.567	1.088	0.041	SIS	1220	78.1	58.0	0.325	7.11	1.645	0.493	No
44	0.444	0.298	0.136	SIS	1220	79.3	58.8	0.089	7.11	1.669	0.386	No
45	0.438	0.716	0.121	SIS	1220	86.3	64.1	0.206	7.11	1.819	0.497	Yes
46	0.312	1.455	0.597	SIS	1220	91.1	67.7	0.410	7.11	1.920	0.602	Yes
47	0.939	0.446	0.024	SIS	1220	86.1	63.9	0.200	7.11	1.814	0.493	No[$]
48	0.864	0.316	0.021	SIS	1220	87.4	64.9	0.126	7.11	1.841	0.457	No[$]
49	0.853	0.389	0.023	SIS	1220	89.0	66.0	0.155	7.11	1.874	0.484	No[$]
50	0.816	0.539	0.034	SIS	1220	89.7	66.6	0.223	7.11	1.889	0.525	No[$]

Table 1 continued

No.	J	F	A (km^2)	Lithology	R_0 (mm)	B (mm)	I (mm)	T	G	R	P	Debris
51	0.844	0.402	0.025	SIS	1220	91.3	67.8	0.162	7.11	1.923	0.501	No[$]
52	0.849	0.511	0.034	SIS	1220	92.6	68.8	0.221	7.11	1.952	0.541	No[$]
53	0.662	0.337	0.060	SIS	1220	91.8	68.1	0.127	7.11	1.933	0.480	No
54	0.711	0.338	0.082	SIS	1220	93.2	69.2	0.145	7.11	1.965	0.501	No[$]
55	0.763	0.356	0.055	SIS	1220	96.0	71.3	0.152	7.11	2.022	0.520	No[$]
56	0.408	0.397	0.161	SIS	1280	99.4	73.8	0.112	7.11	1.997	0.484	Uncertain
57	0.530	0.32	0.089	SIS	1280	101.4	75.3	0.105	7.11	2.036	0.486	Uncertain
58	0.626	0.355	0.081	SIS	1280	103.9	77.2	0.135	7.11	2.087	0.524	Yes
59	0.548	0.362	0.108	SIS	1280	107.0	79.5	0.127	7.11	2.149	0.534	Uncertain
60	0.783	0.66	0.073	SIS	1280	110.2	81.8	0.306	7.11	2.213	0.655	No[$]
61	0.556	0.434	0.110	SIS	1280	113.0	84.0	0.155	7.11	2.272	0.587	Yes
62	0.717	0.457	0.036	SIS	1280	117.5	87.3	0.168	7.11	2.361	0.620	No[$]
63	0.503	0.308	0.070	SIS	1280	117.8	87.5	0.091	7.11	2.367	0.550	Yes
64	0.65	0.314	0.03	SIS	1320	123.8	92.06	0.101	7.11	2.414	0.573	No
65	0.709	0.428	0.031	SIS	1320	124.9	92.86	0.151	7.11	2.435	0.626	Uncertain[$]
66	0.666	0.531	0.053	SIS	1320	128.3	95.4	0.196	7.11	2.502	0.677	Yes

Lithology, T, G, and R are data pertaining to the formation (source) area of the gullies

R_0 the annual precipitation of the site, B cumulative rainfall before the triggering of the debris flows, I the hourly rainfall

[#] SIS: Sandstone interbedded with thin shale (the ratio is about 3–4 to 1)

[$] Average slope in channel is large than 0.7

intensity in the source section of the gully; C_2 is a correction coefficient for tectonics (faults); C_3 is the correction coefficient for physical weathering; C_4 is the correction coefficient for chemical weathering.

The average firmness coefficient for lithology F_0 is based on the Protodyakonov coefficient (Protodyakonov 1962) for rock strength, which was revised after investigations in the field (Yu et al. 2012, 2013a, b, see Table 2). The values of this coefficient for the 66 gullies are the same in the Dayi area: 77.8 % hard siltstone ($F_0 = 8$) interbedded with 22.2 % mudstone ($F_0 = 4$), which gives a weighted average firmness coefficient of $F_0 = 7.11$.

The correction coefficients C_1, C_2, and C_3 (see Eq. 2) of respectively the seismic intensity, tectonics (faults), and physical weathering in the formation area of the gullies are listed in Table 3 (Yu et al. 2012). The correction coefficients C_4 (see Eq. 2) for chemical weathering for the formation area of the gullies are listed in Table 4 (Yu et al. 2013a).

The seismic intensity in the study area is VI, which gives a correction coefficient C_1 of 1 (see Table 3). The correction factor C_2 with respect to the tectonics is 1 because there is no fault in the research area. The physical weathering scores based on the data of the average annual rainfall and temperature in the study area, and the figure of weathering classification with average annual rainfall and temperature are provided by Fookes et al. (1971). The coefficient C_3 for physical weathering in the research area is 1. The chemical weathering is a second factor which plays a role. The intensity of the chemical weathering is controlled by the amount of CO_3^{2-} in rocks such as in limestones, dolomites, etc (see Table 4, Yu et al. 2013a). Chemical weathering in limestone leads to the formation of cracks which hampers the formation of surface runoff (Yu et al. 2013a, b). Therefore, the stronger the chemical weathering, the more difficult it is to form runoff-induced debris flows. So the coefficient C_4 increases with increasing intensity of chemical weathering (see Table 4). As there is no CO_3^{2-} in the rocks of the Dayi area, the coefficient C_4 in the research area is 1. The resulting final geological value for all the 66 gullies is therefore $G = 7.11$ (see Table 1). In the validation areas, we will find more catchments with limestone (see Table 5).

4.3 The rainfall factor

Short-duration high-intensity rainfall is the main triggering factor for the gully-type debris flows (Shieh et al. 2009; Wu et al. 1990; Tan and Han 1992). Yu et al. (2013b) used the 1-h rainfall intensity and cumulative precipitation in the period before the triggering of the debris flow to describe the critical rainfall index for the runoff-induced debris flows.

$$X = B + 12.5I \tag{3}$$

in which X is the critical rainfall index (mm); B is the cumulative precipitation, until the start of the debris flow (mm); I is the amount of rainfall in the hour before the start of the debris flow (mm).

Yu et al. (2013b) used the annual precipitation to normalize the critical rainfall in the Chenyoulan River Watershed. The normalization is very important because rainfall values vary widely between the different areas. The difference may be reduced by introducing a good normalization. Only annual precipitation is not enough to normalize the rainfall. The coefficient of variation represents the local heterogeneity of rainfall. The larger the coefficient of variation, the more heterogeneous is the rainfall. Therefore, the coefficient of

Table 2 The classification of rock types by firmness

Lithology	Firmness coefficient F_0
Basalt, quartzite, peridotite, etc.	14
Gabbro, diorite, andesite, etc.	13
Granite, rhyolite, amphibolite, quartz (siliceous) schist, diabase, quartz-syenite, etc.	12
Dolomite, limestone, gneiss, siliceous slate, marble, conglomerate, etc.	10
Quartz schist, sandy (calcareous, carbonaceous) slate, quartz (siliceous) sandstone, etc.	9
Calcarinate, chalybeate (siliceous, calcareous) siltstone, etc.	8
Phyllite, volcanic tuff, etc.	6
Micacite, marlite, dirtysandstone, argillaceous siltstone, etc.	5
Shale (mud shale, arenaceous shale), mudstone, etc.	4
Soft shale, gupse, calcareous mud shale, anthracite, broken sandstone, lithoid soil, extremely strong weathered granite[#], etc.	2
Broken lithoid soil, broken shale, caking brokenstone, firm coal, hardening clay, etc.	1.5
Sand, gravel, mined coal, etc.	0.5*

[#] $C_3 = 1$

* $G = F_0$, when the solid source are the loose material deposited in the channel, or landslide deposited in the channel

Table 3 Correction factors for seismic intensity, faults (tectonics), and degree of physical weathering

Factor \value	1	0.96	0.93	0.90
Seismic intensity C_1	VI and below	VII	VIII	IX and above
Tectonics C_2	No fault	1 fault	2 faults	3 and more faults
Physical weathering C_3	Mini	Weak	Moderate	Strong

Table 4 Correction factors for degree of chemical weathering

CO_3^{2-} (%)	0	$15 \geq CO_3^{2-} > 0$	$25 \geq CO_3^{2-} > 15$	$35 \geq CO_3^{2-} > 25$	$CO_3^{2-} > 35$
Effect	No	Mini	Weak	Moderate	Strong
Weathering C_4	1.00	1.05	1.10	1.15	1.20

variation was introduced here for the normalization of the rainfall factor in this paper (Ma and Zhang 1991):

$$C_v = \sigma / H \tag{4}$$

in which C_v is the coefficient of variation; σ is the standard deviation of rainfall (mm); H is the average rainfall (mm) over a certain period.

The average rainfall can be calculated over a period of 10 min, 1 h, 6 h, 24 h, and 1 year. So there are corresponding coefficients of variation that can be calculated over these periods. For the same average rainfall, larger amount of rainfall in an area shows always larger coefficients of variation. The coefficient of variation has the same effect as

Table 5 Parametric values related to different debris flow-forming factors and the presence of debris flows in gullies of the validation areas

No.	Region	Name	Time	Lithology	T	G	R	P	Debris	Fr^+	References
1	1	Dayayu G.	Aug.-7-2010	Limestone	0.248	10.29	3.29	0.776	Yes	30	[a]
2	1	Dayayu G.	July-15-1978	Limestone	0.248	10.29	1.59	0.375	Yes	30	[b]
3	1	Dayayu G.	June-18-1982	Limestone	0.248	10.29	1.99	0.469	Yes	30	[b]
4	1	Dayayu G.	May-10-1989	Limestone	0.248	10.29	1.99	0.469	Yes	30	[b]
5	1	Dayayu G.	June-4-1992	Limestone	0.248	10.29	2.04	0.481	Yes	30	[b]
6	1	Dayayu G.	Aug.-7-1994	Limestone	0.248	10.29	1.83	0.432	Yes	30	[b]
7	1	Xiaoyanyu G.	Aug.-7-2010	Limestone	0.243	10.29	3.29	0.773	Yes	30	[a]
8	1	Xiaoyanyu G.	July-15-1978	Limestone	0.243	10.29	1.59	0.374	No	30	[b]
9	1	Xiaoyanyu G.	June-18-1982	Limestone	0.243	10.29	1.99	0.467	No	30	[b]
10	1	Xiaoyanyu G.	May-10-1989	Limestone	0.243	10.29	1.99	0.467	No	30	[b]
11	1	Xiaoyanyu G.	June-4-1992	Limestone	0.243	10.29	2.04	0.497	Yes	30	[b]
12	1	Xiaoyanyu G.	Aug.-7-1994	Limestone	0.243	10.29	1.83	0.43	No	30	[b]
13	1	Luojiayu G.	Aug.-7-2010	Limestone	0.199	10.29	3.29	0.743	Yes	100	[a]
14	1	Luojiayu G.	July-15-1978	Limestone	0.199	10.29	1.59	0.359	No	100	[b]
15	1	Luojiayu G.	June-18-1982	Limestone	0.199	6.24	1.99	0.449	No	100	[b]
16	1	Luojiayu G.	May-10-1989	Limestone	0.199	7.13	1.99	0.449	No	100	[b]
17	1	Luojiayu G.	June-4-1992	Limestone	0.199	7.13	2.04	0.460	No	100	[b]
18	1	Luojiayu G.	Aug.-7-1994	Limestone	0.199	5.89	1.83	0.413	No	100	[b]
19	2	Liuwan G.	June-21-1963	SPL	0.405	0.5[&]	0.299	0.353	Yes	0.1	[c]
20	2	Liuwan G.	July-10-1963	SPL	0.405	0.5[&]	0.327	0.386	Yes	0.1	[c]
21	2	Liuwan G.	July-6-1963	SPL	0.405	0.5[&]	0.368	0.434	Yes	0.1	[c]
22	2	Liuwan G.	July-24-1963	SPL	0.405	0.5[&]	0.363	0.428	Yes	0.1	[c]
23	2	Liuwan G.	Aug.-14-1963	SPL	0.405	0.5[&]	0.295	0.348	Yes	0.1	[c]
24	2	Liuwan G.	Aug.-20-1963	SPL	0.405	0.5[&]	0.405	0.478	Yes	0.1	[c]
25	2	Liuwan G.	Aug.-29-1963	SPL	0.405	0.5[&]	0.455	0.537	Yes	0.1	[c]

Table 5 continued

No.	Region	Name	Time	Lithology	T	G	R	P	Debris	Fr^{+}	References
26	2	Niwan G.	July-7-1965	SPL	0.177	0.5[&]	0.653	0.653	Yes	0.2	c
27	2	Niwan G.	July-19-1965	SPL	0.177	0.5[&]	0.429	0.429	Yes	0.2	c
28	2	Niwan G.	July-20-1965	SPL	0.177	0.5[&]	0.413	0.413	Yes	0.2	c
29	2	Huoshao G.	June-13-1963	SPL	0.262	0.5[&]	0.426	0.461	Yes	0.5	c
30	2	Huoshao G.	Aug.-26-1972	SPL	0. 262	0.5[&]	0.620	0.671	Yes	0.5	c
31	2	Huoshao G.	June-12-1973	SPL	0. 262	0.5[&]	0.821	0.888	Yes	0.5	c
32	3	Wenjia G.	Sep.-24-2008	Limestone	0.193	0.5[$]	0.626	0.637	Yes	0.5	d
33	3	Wenjia G.	July-31-2010	Limestone	0.193	0.5[$]	1.027	1.045	Yes	0.5	d
34	3	Wenjia G.	Aug.-13-2010	Limestone	0.193	0.5[$]	1.487	1.513	Yes	0.5	d
35	3	Wenjia G.	Aug.-19-2010	Limestone	0.193	0.5[$]	0.640	0.652	Yes	0.5	d
36	3	Wenjia G.	Sep.-18-2010	Limestone	0.193	0.5[$]	0.576	0.586	Yes	0.5	d
37	4	Luwan G.	Nov.-2-1979	Sandstone	0.048	7.14	2.054	0.419	Yes	100	e
38	4	Luwan G.	–	Sandstone	0.048	7.14	1.908	0.389	No	100	e
39	4	Ganxi G.	Nov.-2-1979	Sandstone	0.062	7.14	2.054	0.441	Yes	100	e
40	4	Ganxi G.	–	Sandstone	0.062	7.14	1.908	0.409	No	100	e
41	4	Lengmu G.	Aug.-18.2012	LSL	0.197	6.51	1.885	0.534	Yes	25	f
42	4	Jiaochang G.	Aug.-18-2012	Limestone	0.343	9.64	1.885	0.490	Yes	25	f
43	5	Aizi G.	June-28-2012	BSM	0.226	8.03	2.087	0.547	Yes	50	g
44	5	Diwan G.	Aug.-24-2004	DD	0.129	8.65	1.465	0.331	No	60	h
45	5	Hupiwan G.	Aug.-24-2004	DS	0.151	8.86	1.414	0.326	Yes	60	h
46	5	Dawan G.	Aug.-24-2004	DS	0.103	9.18	1.515	0.318	No	60	h
47	5	Shijiawan G.	Aug.-24-2004	DS	0.136	10	1.519	0.322	No	60	h
48	5	Huangjiawan G.	Aug.-24-2004	Phyllite	0.173	5.58	1.571	0.468	No	40	h
49	5	Wenjia G.	Aug.-24-2004	DS	0.197	5.36	1.587	0.496	Yes	40	h
50	5	Yinchang G.	Aug.-24-2004	SP	0.202	6.42	1.605	0.460	No	40	h

Table 5 continued

No.	Region	Name	Time	Lithology	*T*	*G*	*R*	*P*	Debris	Fr[+]	References
51	5	Lao G.	Aug.-24-2004	DPD	0.136	7.35	1.562	0.386	No	40	[h]
52	5	Mujia G.	Aug.-24-2004	SPA	0.123	5.02	1.738	0.510	Yes	40	[h]
53	5	Aomiluo G.	Aug.-24-2004	PA	0.147	4.65	1.782	0.563	Yes	20	[h]
54	5	Liangfeng G.	Aug.-24-2004	GED	0.138	4.84	1.467	0.449	Yes	20	[h]
55	5	Yanjia G.	Aug.-24-2004	GED	0.101	5.04	1.518	0.427	Yes	20	[h]
56	5	Xiejia G.	Aug.-24-2004	GED	0.111	5.04	1.621	0.465	Yes	20	[h]
57	5	Guanjia G.	Aug.-24-2004	GED	0.127	5.04	1.666	0.491	Yes	20	[h]
58	5	Huangjiao G.	Aug.-24-2004	GED	0.141	4.84	1.708	0.525	Yes	20	[h]
59	5	Gaidong G.	Aug.-24-2004	GED	0.179	4.84	1.760	0.567	Yes	20	[h]
60	5	Wayao G.	Aug.-24-2004	GE	0.117	10.7	1.781	0.355	No	60	[h]

Lithology, T, G, and R are data pertaining to the formation (source) area of the gullies

SPL shale, phyllite, and limestone, *LSL* limestones, shales with alternating siltstones, limestones with alternating mudstones, *BSM* basalt, siltstone and thin mudstone, *DD* dolomite and dirtysandstone, *DS* dolomite and siltstone, *SP* siliceous siltstone and phyllite, *DPD* dolomite, phyllite, and dirtysandstone, *SPA* siltstone, phyllite, and argillaceous siltstone, *PA* phyllite and argillaceous siltstone, *GED* granite, extremely strong weathered granite, diabase, *GE* granite, and diabase

[+] Fr: Return period in years

[&] Landslide deposited in the channel

[$] Landslide debris deposited in the channel caused by Wenchuan earthquake

[a] Yu et al. (2010)

[b] Ma and Qi (1997)

[c] LIGC and TSIG (1982)

[d] Yu et al. (2013a)

[e] Tan and Yang (1984)

[f] This study

[g] Hu et al. (2012)

[h] This study and Su et al. (2010)

the annual precipitation: the larger the coefficient of variation and annual precipitation, the larger the rainfall threshold.

Wu et al. (1990) indicated that the 10-min rainfall intensity is strongly correlated with the triggering of debris flows with a runoff-induced mechanism. Although we use here the 1-h rainfall intensities (Eq. 3), it is better to use for the normalization the coefficient of variation of 10 min instead of the coefficient of variation of 1 h. Therefore, we normalized the critical rainfall with the annual precipitation and the coefficient of variation of 10 min (when available) to obtain the dimensionless rainfall factor R (Eq. 5):

$$R = \frac{X}{R_0 C_v} = \frac{B + 12.5I}{R_0 C_v} \tag{5}$$

in which R is the dimensionless rainfall factor; R_0 is the annual precipitation of the site (mm); C_v is the coefficient of variation of 10 min. The annual precipitation R_0 for each gully is obtained from the spatial distribution of the annual rainfall in the study area by the interpolation of the rainfall data of the Dayi and Xintun stations. In the Dayi area, only the coefficient of variation for a 24-h period ($C_v = 0.45$) and a 1-h period ($C_v = 0.4$) is available. So we were obliged to use in the Dayi test area the coefficient of variation for 1 h instead of the 10-min coefficient of variation: $C_v = 0.4$. The values of the hydraulic factor R for all the 66 gullies are listed in Table 1.

5 The calibration of the prediction model in the Dayi area and the validation in some areas of southwest China

5.1 Model calibration in the Dayi area

Yu et al. (2013b) obtained a formation model with data of debris flows with a runoff-induced mechanism in the Chenyulan River watershed (Taiwan) triggered during the Typhoon Toraji. With the refined geological factor given by Yu et al. (2013a) and the rainfall factor proposed in this study, a prediction model for debris flows with a runoff-induced mechanism is obtained using the data of the rainstorm event from June 5 to June 6, 2011, in the Dayi region. The prediction factor P can be expressed by T (Eq. 1), G (Eq. 2), and R (Eq. 5) (Yu et al. 2013b) as in Eq. 6 by empirical statistic analyses:

$$P = RT^{0.2}/G^{0.5} \geq C_r \tag{6}$$

in which P is the prediction factor; C_r is a critical value for the prediction of debris flows.

The values for the prediction factor P for all the 66 gullies are listed in Table 1. Figure 3 shows a scatter plot of R against $T^{0.2}/G^{0.5}$ (from Eq. 6) for all the 66 gullies and two graphs for two different values of P, marking two critical probability values for debris flow prediction. All the debris flows lie beyond the critical line $C_{r1} = 0.35$ in Fig. 3, while 80 % of the debris flows lie beyond the line, $C_{r2} = 0.47$. These critical boundaries deliver a subdivision into three classes of the probability of debris flow occurrence. Debris flows are hardly formed in the area with $P < 0.35$. This area can be considered as a *very low probability* or safe area. Some debris flows (5 out of a total of 25, 20 %) are formed in the area between $0.35 \leq P < 0.47$, which makes this area a *medium probability* or an alarm area. When $P \geq 0.47$, debris flows are triggered in most gullies (20 out of 25, 80 %), which makes it a *high-probability* area. In this area, people have to be evacuated to safer places.

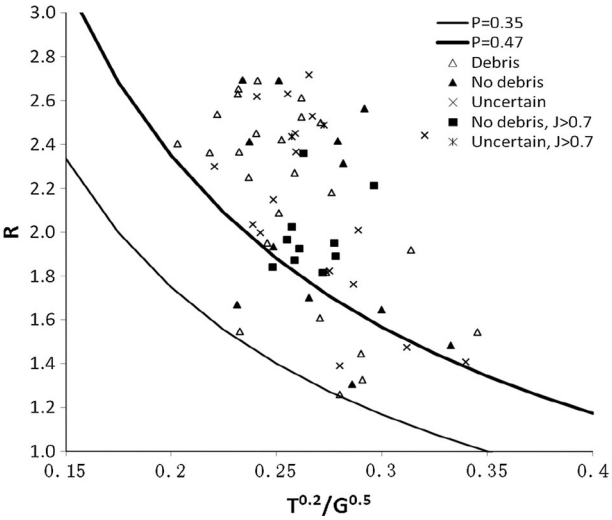

Fig. 3 The critical lines for the probability of debris flow occurrence in the calibration area of Dayi. $J > 0.7$ means gullies with steep channels (>35°) without source material for debris flows

5.2 Validation in southwest China

Also, in southwest China, many debris flows are triggered every year with a runoff-induced mechanism. Some of them cause enormous damage and many casualties (Yu et al. 2010). Figure 4 shows the location of five regions with debris flows in southwest China. The topographic, geological, and rainfall factors in the gullies of these regions are quite different (see Table 5): The topographic factor ranges from 0.048 to 0.405, the geological factor from 0.5 to 10.29, and the rainfall factor from 0.295 to 3.29 (the annual precipitation varies between 410 and 1,718 mm, and the 10-min rainfall coefficient of variation between 0.35 and 0.73). The value of $T^{0.2}/G^{0.5}$ for the investigated gullies is concentrated between 0.2 and 0.4, and between 1.0 and 1.2 (see Fig. 5). The difference in debris flow frequency is also very large (see Table 5). In the range of $T^{0.2}/G^{0.5}$-values between 1.0 and 1.2, the debris flows may occur several times each year in one location, while for $T^{0.2}/G^{0.5}$-values between 0.2 and 0.4, the frequency is only once in 10 years.

Equation 6 and Figs. 3 and 5 show us how the critical rainfall threshold R for a certain catchment is controlled clearly by the topographic (T) and lithological characteristics (G) of the catchment. The predictive factors (T, G, and R) and the final predictive score P are listed in Table 5 for the different areas.

Figure 5 shows the validation of the prediction model for the selected areas in southwest China. All the points beyond the line of $P \geq 0.47$ are debris flows. Almost all the points with debris flows are located in the domain $P \geq 0.35$, and more than half of these points are located in the domain $P \geq 0.47$ (see Table 6). So the two critical P lines subdivide classes with almost the same probability in the Dayi area and areas in southwest China. The prediction model obtained from data of a rain event with debris flows around Dayi, in the Guizhou Province, is applicable in other areas in the southwest of China and may be also a good predictor in other areas.

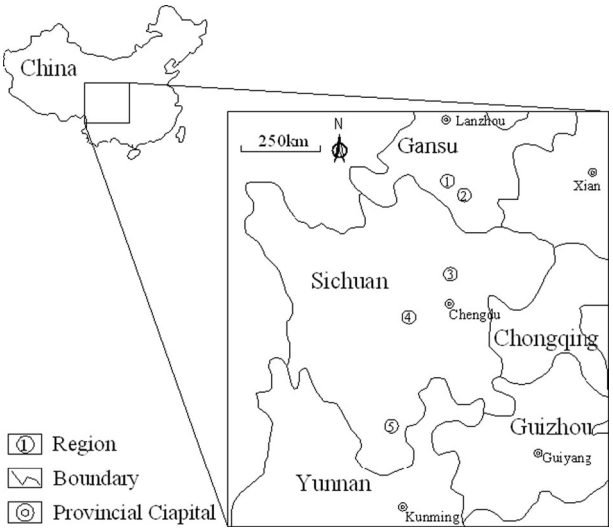

Fig. 4 The validation regions in southwest China

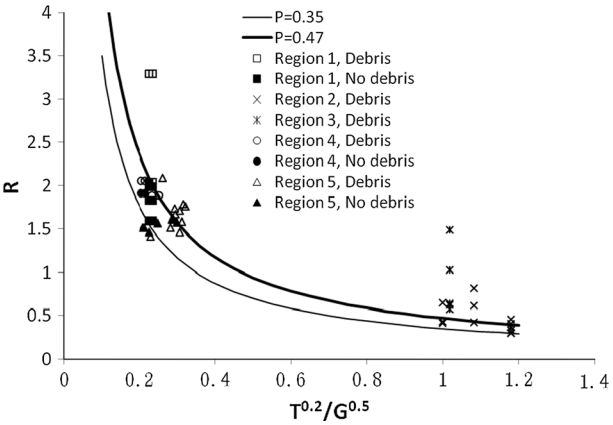

Fig. 5 The validation of the prediction model for debris flows in different regions of southwest China

Table 6 The percentages of debris flow (DF) and no debris flow (no DF) in the three classes

Percentage of DF or No DF	Dayi: DF (%)	Dayi: No DF (%)	SW China: DF (%)	SW China No DF (%)
$P < 0.35$	0	0	5	16
$0.35 \leq P < 0.47$	20	25	39	84
$P \geq 0.47$	80	75	56	0

6 Discussion

Landslides, channel bed erosion, and destruction of natural dams are three common causes that trigger debris flows (Takahashi 2000). In this study area, only the runoff-induced mechanism (channel bed erosion) is considered as the trigger mechanism of debris flows in the study area. The prediction factor P is not suitable for the other mechanisms of debris flow formation.

In 2011, a heavy rainstorm that occurred in the Dayi area (Guizhou Province) provided an unprecedented amount of data to establish a model for the prediction of debris flows with a runoff-induced mechanism. For our revised prediction model proposed in this study, we had to include the category "uncertain" for gullies where the triggering mechanism of the debris flows was not sure. Neglecting the impact of these uncertain cases in the results, the distinction of the probability of occurrence of debris flows by means of the prediction factor P is acceptable despite the fact that some gullies with no debris flows are found in the domain with very high probability, and no data in the domain $P < 0.35$. The validation of the prediction model in southwest China was reasonable good withstanding the fact that the characteristics of these gullies are quite different to those of the calibration area. In the high-probability domain ($P \geq 0.47$) of the Dayi events, there are still some gullies with the absence of debris flows. Some of these gullies have very steep channel gradients in the formation (source) area: $J > 0.7$ (35°). Since the angle of repose of rock particles is around 35° (Yang et al. 2009), one can hardly expect sediment deposits in such steep channel sections which means there is no source material for debris flow development. Therefore, the channel gradient J for the topographic factor (Eq. 1) is only valid for $J \leq 0.7$. The points with "No debris, $J > 0.7$" and "Uncertain, $J > 0.7$" in Fig. 3 represent unrealistic (false) values because the debris flow cannot take place whatever the values of the geological and rainfall factor. This hypothesis needs to be proved in future research.

Without the "false" data, there are still nine gullies with the absence of debris flows in the high-probability area ($P \geq 0.47$) during the Dayi events. This study cannot explain why no debris flows were triggered in these gullies. Future work is needed to give an explanation for these cases.

Some rainstorm events produce extreme values for the rainfall factors leading to P-values far above the critical value $P = 0.47$. For example, the rainfall event of Zhouqu on August 7, 2010, causing the death of 1,744 people (Yu et al. 2010), produced P-values in the range of 0.743–0.776 and huge debris flows in the catchments. Another extreme case is the rainfall event in the Wenjia Gully on August 13, 2010 (Yu et al. 2013c), which produced 3.1 million cubic meters of debris flow material, with a P value of 1.513. Lower debris flow volumes were produced in the same catchment with a P-value near the critical value (see Table 7). Figure 6 shows the exponential relationship ($R^2 = 0.93$) between P-values and related dimensionless debris flow volumes S expressed by Eq. 7:

$$S = 0.07e^{2P} - 0.14 \tag{7}$$

$$S = \frac{V}{AR_0C_v} \tag{8}$$

in which S is the dimensionless volume of a debris flow; V is the volume of a debris flow (m^3); A is the area of the formation section of the gully (m^2); R_0 is the annual precipitation of the site (m); and C_v is the 10-min coefficient of variation.

The only outlier in Fig. 6 is the debris flow, which occurred in the Wenjia Gully on July 31, 2010. The predicted volume is much higher than the observed volume because the

Table 7 Some gullies with *P*-values and debris flow volumes

Gully name	Time	*P*	*V* (10^6 m^3)	R_0 (m)	C_v	*A* ($10^6 m^2$)	*S*	References
Dayayu G.	Aug.-7-2010	0.776	0.732	0.436	0.73	8.68	0.265	[a]
Dayayu G.	June-4-1992	0.481	0.106	0.436	0.73	8.68	0.038	[b]
Xiaoyanyu G.	Aug.-7-2010	0.773	0.353	0.436	0.73	7.36	0.151	[a]
Xiaoyanyu G.	June-4-1992	0.497	0.164*	0.436	0.73	7.36	0.070	[b]
Wenjia G.	Sep.-24-2008	0.637	0.500	1.500	0.40	3.97	0.210	[c] and d
Wenjia G.	July-31-2010	1.045	0.200	1.500	0.40	3.97	0.084	[c] and [d]
Wenjia G.	Aug.-13-2010	1.513	3.100	1.500	0.40	3.97	1.301	[d]
Wenjia G.	Aug.-19-2010	0.652	0.300	1.500	0.40	3.97	0.126	[c] and [d]
Wenjia G.	Sep.-18-2010	0.586	0.170	1.500	0.40	3.97	0.071	[c] and [d]
Lengmu G.	Aug.-18.2012	0.534	0.219	1.102	0.375	5.71[@]	0.093	e
Jiaochang G.	Aug.-18-2012	0.490	0.0145	1.102	0.375	1.75[#]	0.020	e
Aizi G.	June-28-2012	0.547	0.300	0.769	0.3	9.18	0.194	f

* Deduce from the data of Ma and Qi (1997)

[@] Areas of all subarea of presence of debris flows

[#] Areas of all subarea of presence of debris flows

[a] Yu et al. 2010

[b] Ma and Qi 1997

[c] Xu 2010

[d] Yu et al. 2013c

[e] This study

[f] Hu et al. (2012)

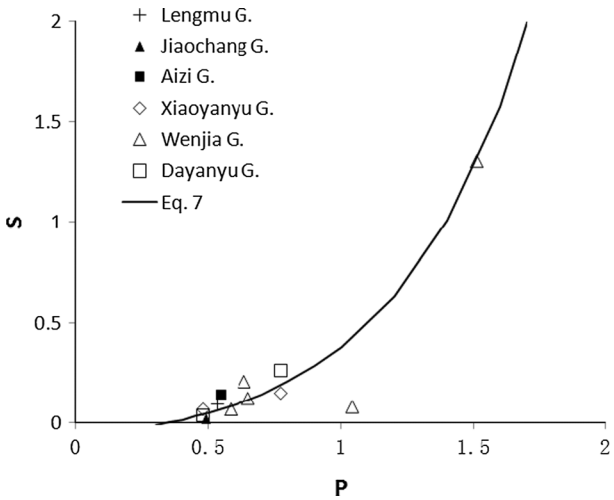

Fig. 6 The relationship between the *P* value and a dimensionless volume *S* of debris flows

debris flow prevention works kept most of the sediment behind the last dam of the Wenjia Gully (Xu 2010; Xu et al. 2012). We can conclude that the prediction model may not only forecast the probability of occurrence of debris flows, but also the scale of the debris flows.

The area A (see Eq. 8) of the formation section varies in the data set between 0.1 and 100 km^2. However, we have only a limited amount of rainfall data in combination with related debris flow volumes to set up the relationship given in Eq. 7 and depicted in Fig. 6. The areas A (Eq. 8) of these gullies have in addition a narrow range between 1.75 and 9.18 km^2. Therefore, more work should be conducted to verify Eq. 7.

In this study, many lithologies were involved in the determination of the geological factor in the Dayi area and the five regions of southwest China. It appeared that we had to introduce a low firmness coefficient values for very soft and loose materials in order to forecast the high sensitivity for debris flows in these catchments. For example, in the Hunshui Gully, debris flows were triggered many times within 1 year (Zhang and Liu 1989). This is caused by the presence in this gully of extremely strong weathered granite which we found during our field investigations. So a low value of 2 was given for the average firmness coefficient F_0 of this extremely strong weathered granite (see Table 2).

Han et al. (2011) divided the frequency of debris flows in gullies in 4 classes: extremely high: occurring several times each year; high: occurring once in 1–5 years; medium: occurring once in 5–20 years; and low: occurring once in 20 years or more. The return periods (in years) of debris flows in southwest of China are shown in Table 5. Figure 7 shows the relationship between the return period (frequency) and geological factor G-value, and $T^{0.2}/G^{0.5}$-value of debris flows. Figures 5 and 7 show debris flow gullies with a $T^{0.2}/G^{0.5}$-value within the range of 1.0–1.2. These gullies have a minimum geological factor ($G = 0.5$) with a low firmness coefficient (0.5) because these catchments are filled with plenty of fine sediments. The debris flow may occur several times each year in one location and are therefore high-frequency debris flow gullies. Figure 5 shows also gullies with a value of $T^{0.2}/G^{0.5}$ in the range of 0.2–0.4, with much higher G values such as limestone (10.29), sandstones (7.14), granite and diabase (10.7), etc (see Fig. 7). These gullies may be low-frequency debris flow gullies (20 years or more). No data were collected in this study for $T^{0.2}/G^{0.5}$-values in the range of 0.4–1.0 (See Figs. 5, 7). The frequency of debris flows within this range may be once in 5–20 year (medium) or once in 1–5 year (high). From the relationship between frequency and $T^{0.2}/G^{0.5}$-values and G-values, one can conclude that the debris flow activity in gullies may be determined by the topographic and geological factors, or only by the geological factor. But that have to be verified by future studies with new data.

The runoff-induced effect may be more related to short-duration rainfall intensity. Kean et al. (2011) pointed that the post-fire debris flow stage was best cross-correlated with time series of 5-min rainfall intensity and lagged the rainfall by an average of just 5 min. Wu et al. (1990) indicated that the 10-min rainfall intensity is strongly correlated with the triggering of the runoff-induced debris flows. In this paper, we suggest to use for the normalization the coefficient of variation of 10 min instead of the coefficient of variation of 1 h. It may be better to use the 10-min rainfall factors instead of the 1-h rainfall factors. Unfortunately, it is difficult to obtain the information of 10-min intensities. We have to use the 1-h rainfall factors in this paper. To get better results of the prediction of debris flows with a runoff-induced mechanism, 10-min rainfall intensity should be used in future research.

The critical value C_{r2} is 34.3 % higher than the critical value C_{r1} (Eq. 6), which shows a moderate performance of the prediction model. For a more accurate prediction of the occurrence of debris flows, more research is needed to reduce the difference between C_{r1} and C_{r2}.

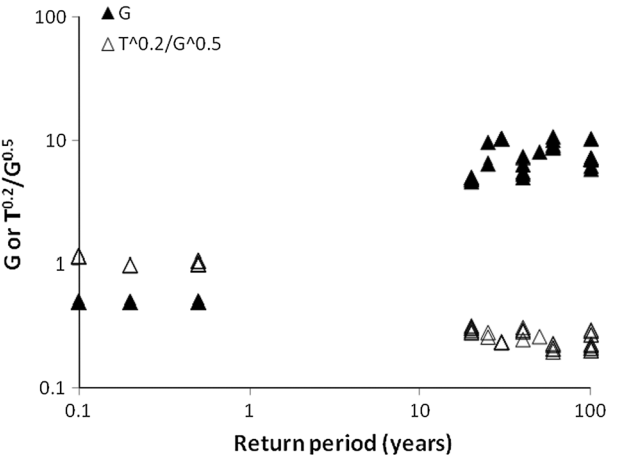

Fig. 7 The relationship between the return period (frequency) and geological factor G, and $T^{0.2}/G^{0.5}$ of debris flows

7 Conclusions

The heavy rainstorm from June 5 to June 6, 2011, caused a severe debris flow activity in the Dayi area, Guizhou Province, China. Short-duration high-intensity rainfall was the main triggering factor for these gully-type debris flows with a runoff-induced mechanism. This research proposed a prediction model for debris flows based on a refined, geological, and rainfall factor. These dimensionless factors are not totally deduced from the statistical analyses of a given area but partly based on the mechanism for the formation of debris flows. The model was calibrated on the June 5–6 storm event in the Dayi area. The prediction model has a generic nature, because it could be validated with reasonable success in other areas of southwest China with complete different gully characteristics.

In our view, the prediction model offers a new and exciting way to forecast the probability of occurrence of the runoff-induced debris flows. However, to improve the understanding of the occurrence and triggering mechanisms of debris flows, future research is needed to include the effect of large channel gradients, to discover the reason for the miss-classification of the absence of debris flows in the high-probability domain (large P-value), to prove the usability of the model in areas with a medium and high debris flow activity, and to reduce the difference between critical probability values.

Acknowledgments This work was supported by the National Natural Science Foundation of China (NSFC, contract number: 41372366) and the State Key Laboratory of Geohazard Prevention and Geoenvironment Protection Foundation (contract number: SKLGP2012Z011). We thank the reviewers for their comments that helped us to greatly improve the presentation of this work. We are grateful to Dr. Theo van Asch for having provided a very helpful review of the manuscript, and for help on the English editing of the manuscript.

References

Cannon SH, Gartner JE, Rupert MG, Michael JA, Rea AH, Parrett C (2010) Predicting the probability and volume of postwildfire debris flows in the intermountain western United States. Geol Soc Am Bull 122(1–2):127–144

Chang TC (2007) Risk degree of debris flow applying neural networks. Nat Hazards 42:209–224

Fookes PG, Dearman WR, Franklin JA (1971) Some engineering aspects of rock weathering with field examples from dartmoor and elsewhere. Q J Eng Geol 4(3):161–163

Han L, Yu B, Lu K (2011) Relationship of frequency of debris flows and the particle size in the channel. Res Environ Yangtze Basin 20:1149–1156 (in Chinese with English abstract)
Hu K, Cui P, Ma C, Zhou G, Tian M (2012) Causes and characteristics of 28 June disastrous debris flow event in Ningnan County of Sichuan, China. J Mt Sci 30(6):696–700 (in Chinese with English abstract)
Johnson AM, Rodine JR (1984) Debris flow. In: Brunsden D, Prior DB (eds) Slope instability. Wiley, Chichester, UK, pp 257–361
Kean JW, Staley DM, Cannon SH (2011) In situ measurements of post-fire debris flows in southern California: comparisons of the timing and magnitude of 24 debris-flow events with rainfall and soil moisture conditions. J Geophys Res 116:F04019. doi:10.1029/2011JF002005
Kean JW, McCoy SW, Tucker GE, Staley DM, Coe JA (2013) Runoff-generated debris flows: observations and modeling of surge initiation, magnitude, and frequency. J Geophys Res Earth Surf 118:2190–2207
LIGC and TSIG (Lanzhou Institute of Glaciology and Cryopedology, and Traffic Science Institute of Gansu Province, China) (1982) Debris flow in Gansu Province. People's Transportation Press, Beijing, pp 125–156
Liu C, Dong J, Peng Y, Huang H (2009) Effects of strong ground motion on the susceptibility of gully type debris flows. Eng Geol 104(3–4):241–253
Ma D, Qi L (1997) Study on comprehensive controlling of debris flow hazard in Sanyanyu Gully. Bull Soil Water Conserv 17(4):26–31 (in Chinese with English abstract)
Ma S, Zhang X (1991) Some rules of variation coefficient of annual rainfall in Xinjiang. ACTA Meteorol SINICA 49(1):39–45 (in Chinese with English abstract)
NSBC (National Seism Bureau of China) (1990) Seismic distribution map of China. Beijing, Seism Press. (in Chinese)
Protodyakonov MM (1962) Mechanical properties and drillability of rocks. In: Proceedings of the fifth symposium on rock mechanics. Minneapolis, MN, University of Minnesota, pp 103–118
Shieh CL, Chen YS, Tsai YJ (2009) Variability in rainfall threshold for debris flow after the Chi–Chi earthquake in central Taiwan, China. Int J Sedim Res 24:177–188
Su P, Wei F, Gu L, Ni H (2010) Characteristic and causes of group-occurring debris flow in Dechang County, Sichuan Province. J Mt Sci 28(5):593–606 (in Chinese with English abstract)
Takahashi T (2000) Initiation and flow of various types of debris flow. In: Wieczorek GF, Naeser ND (eds) Debris-flows hazard mitigation: mechanics, prediction, and assessment balkema. Rotterdam, Netherlands, pp 15–25
Tan W, Han Q (1992) Research on the critical rainfall of debris flows in Sichuan Province, China. Hazards 7(2):37–42 (in Chinese with English abstract)
Tan W, Yang Z (1984) "791102" debris flows of Yaan and analysis of torrential rain genesis. Debris Flow (No.3). Chongqin: Chongqin division of Science and Technique Press, pp 9–14 (in Chinese with English abstract)
Wu J, Kang Z, Tian L, Zhang S (1990) Observation and research on the debris flows in Jiangjia Gully, Yunnan Province, China. Science Press, Beijing, pp 197–221
Xu Q (2010) The 13 August 2010 catastrophic debris flow in Sichuan Province: characteristics, genetic mechanism and suggestions. J Eng Geol 18:596–608 (in Chinese with English abstract)
Xu Q, Zhang S, Li L, van Asch ThWJ (2012) The 13 August 2010 catastrophic debris flows after the 2008. Nat Hazards Earth Syst Sci 12:201–216
Yang F, Liu X, Yang K, Cao S (2009) Study on the angle of repose of nonuniform sediment. J Hydrodyn 21:685–691
Yu B, Yang Y, Su Y, Huang W, Wang G (2010) Research on the giant debris flow hazards in Zhouqu County, Gansu Province on August 7, 2010. J Eng Geol 18:437–444 (in Chinese with English abstract)
Yu B, Li L, Ma Y, Zhang J, Wu Y, Zhang H, Chu S, Qi X (2011) Research on topographical factors in the formation of gully type debris flows. River, coastal and estuarine morphodynamics: RCEM2011, Tsinghua University Press, Beijing, pp 1–10
Yu B, Chu S, Lu K, Han L, Xie H (2012) A study about the relationship between the frequency of debris flows and lithology. In: Eberhardt et al (ed) Landslides and engineered slopes: protecting society through, improved understanding, pp 757–761
Yu B, Chu S, Zhu Y, Xie H (2013a) Impacts of weathering on formation of gullied debris flow. Bull Soil Water Conserv 33:51–56 (in Chinese with English abstract)
Yu B, Li L, Wu Y, Chu S (2013b) A formation model for debris flows in the Chenyulan River Watershed, Taiwan. Nat Hazards 68:745–762
Yu B, Ma Y, Wu Y (2013c) Case study of a giant debris flow in the Wenjia Gully, Sichuan Province, China. Nat Hazards 65:835–849
Zhang X., Liu J (1989) Debris flows in the basin of Dayinjaing, Yunnan, China. Chengdu, Map Press of Chengdu, pp 1–64. (in Chinese)